Investigation on Fluorescence Properties of Ultrafine PVA Fiber Mats-Contained Polyoxometalate with Different Molecular Structure

Yongling Sun, Yuping Shan, Xiujun Cui, Bin Li, Jian Gong, Zhongmin Su, Lunyu Qu

Key Laboratory of Polyoxometalates Science of Ministry of Education, Northeast Normal University, Changchun 130024, People's Republic of China

Received 15 June 2007; accepted 14 February 2008
DOI 10.1002/app.30086
Published online 14 April 2009 in Wiley InterScience (www.interscience.wiley.com).

ABSTRACT: Novel luminescence ultrafine fiber mats containing $K_{11}[Eu(PW_{11}O_{39})_2]$ [$EuPW_{11}$] and $Na_9[EuW_{10}O_{36}]$ [EuW_{10}] entrapped in polyvinyl alcohol (PVA) have been successfully prepared by electrospinning method. By comparing the luminescence emission spectra of $EuPW_{11}$/PVA and EuW_{10}/PVA ultrafine fiber mats, we conclude lower site symmetry of Eu^{3+} in the $EuPW_{11}$/PVA ultrafine fiber mats. We further investigate the different configurations of $EuPW_{11}$ and EuW_{10}, which lead to the different site symmetry of Eu^{3+} in the ultrafine fiber mats of $EuPW_{11}$/PVA and EuW_{10}/PVA. Fluorescence property shows $EuPW_{11}$/PVA ultrafine fiber mats display pure red emission. © 2009 Wiley Periodicals, Inc. J Appl Polym Sci 113: 1369–1374, 2009

Key words: fluorescence; configuration; polyoxometalate; lanthanide; fiber mats; electrospinning

INTRODUCTION

Transition metal substituted polyoxometalates (POMs), as a well-known class of well-defined clusters with an enormous variation in size, metal-oxygen framework topology, composition, and function.[1,2] In recent years, POMs have attracted widespread attentions because of the structural variety as well as interesting properties and often unexpected physical and chemical properties in fields as diverse as catalysis, medicine, biology, electrochemistry, photophysics, magnetics, materials science, and even heavy construction.[3–5] POMs can offer unique functionality when combined with lanthanide (Ln) ions by binding to surface bridging or terminal oxygen atoms.[6,7] Ln cations-substituted POMs have been found display excellent luminescence properties and have been prove to be good candidate for various electronic, magnetic, Lewis acid catalytic centers, especially for luminescent materials. So far, a great deal of publications have demonstrate the fabrication of photoluminescence multibilayer Ln cations-substituted POMs composite films by various effective and convenient methods, for example, the ion-exchange method,[8] consecutive layer-by-layer electrostatic adsorption,[9–11] Langmuir-Blodgett technique,[12] sol-gel process,[13] dip-coating method.[14] However, all the reports focus mainly on confirming the potential for creating photoluminescence multibilayer with POMs but not give detailed investigations on different photoluminescence behavior due to the different configurations of POMs.

Our group has done much work on prepared photoluminescence ultrafine fibers based on rare earth substituted polyoxometalates via electrospinning method. In this article, we report the preparation of ultrafine fiber mats containing polyoxotungstoeuropate with Keggin-like $K_{11}[Eu(PW_{11}O_{39})_2]$ and $Na_9[EuW_{10}O_{36}]$ entrapped in polyvinylalcohol (PVA) using electrospinning technique. IR, UV–vis spectra, and SEM image characterize the structure of the ultrafine fiber mats. The experiment results indicate that the $EuPW_{11}$/PVA hybrid ultrafine fiber mats have good photoluminescence behaviors. By comparing the luminescence of $EuPW_{11}$/PVA and EuW_{10}/PVA hybrid ultrafine fiber mats, we find that different polytungstates ligands arose different photoluminescence behavior of Eu^{3+} in hybrid ultrafine fiber mats.

EXPERIMENTAL

Experimental materials and apparatus

$EuPW_{11}$ and EuW_{10} (Eu-POMs) were prepared according to Refs. [15] and [16], respectively. The molecular formulas were confirmed on the basis of IR

Correspondence to: J. Gong (gongj823@nenu.edu.cn).
Contract grant sponsor: Program for Changjiang Scholars and Innovative Research Team in University and the Science Foundation of Jilin Province; contract grant number: 20070505.

Journal of Applied Polymer Science, Vol. 113, 1369–1374 (2009)

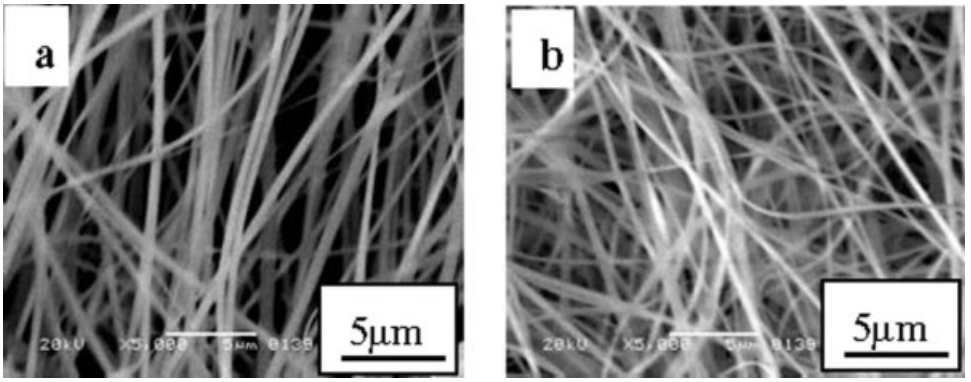

Figure 1 SEM photograph of the ultrafine fiber mats of the $EuPW_{11}$/PVA (a) and EuW_{10}/PVA (b) prepared by electrospinning technique.

spectrum. The other chemicals used were of analytical grade.

IR studies were carried out on Impact 410 FT-IR spectrophotometer in the range of 500–4000 cm^{-1} with fiber mats. The UV–vis absorption spectra were obtained with Beckman-DU-8B UV spectrophotometer. Fluorescence spectra were measured on a Spex FL-2T2 spectrophotometer using a xenon lamp as excitation source. For scanning electron microscope (SEM) investigation, an Amray 3000 SEM was used.

Preparation of the ultrafine fiber mats

Aqueous PVA (M_n, 86,000) solution was prepared by dissolving 1 g of PVA powder in 9 g of distilled water under vigorous stirring at 90°C. After about 5 h of stirring, a transparent solution was obtained. Then the solution was cooled to room temperature. The synthesis of $EuPW_{11}$/PVA composite is described as follows: 10 g of PVA solution was added to 0.33 g solid of $EuPW_{11}$. The solution was stirred vigorously for 4 h at room temperature, and then the homogeneous and transparent PVA solution contained $EuPW_{11}$ was obtained.

The $EuPW_{11}$/PVA solution was contained in a medical syringe fixed with a size 10-cm metal needle. The needle was connected to a high-voltages supply. In our experiment, a voltage of 15 kV was applied to the solution for electrospinning. The syringe was tilted downward at an angle about 30°. The ultrafine fiber mats were collected on a flat aluminium foil, which was placed 20 cm from the tip of the needle and dried under vacuum for 24 h at 40°C. The EuW_{10}/PVA ultrafine fiber mats were obtained by the same way.

RESULT AND DISCUSSION

SEM photograph

Figure 1 shows SEM micrographs of the Eu-POMs/PVA ultrafine fiber mats. The shape of the Eu-POMs/PVA hybrid materials are composed of the ultrafiber mats with random oriented nanometer-scale. The diameter of the ultrafine fiber mats are found to be in the range of 200–600 nm. Fibers collected on the flat aluminium foil show smooth surface without droplet.

IR spectra

Figure 2 shows IR spectra of the pure solid and ultrafine fiber mats. In the IR spectra of Eu-POMs/PVA ultrafine fiber mats, the broad band around 3400 and 1429 cm^{-1} are associated with O—H stretching and bending, which are assigned to stretching mode of water and PVA. Several characteristic bands of PVA appear at about 2933 cm^{-1} (C—H bands) and 1090 cm^{-1} (C—O band).[17–19] Besides those bands, the IR spectra show very strong bands below 1200 cm^{-1}, due to the Eu-POMs.[20] There are four kinds of oxygen atoms in the Eu-POMs, i.e., O_a (oxygen in PO_4 tetrahedron), O_b (corner-sharing oxygen between different

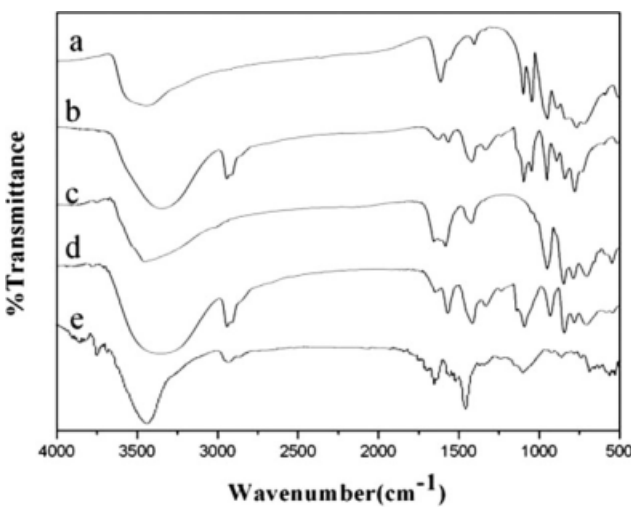

Figure 2 IR spectra of samples: (a) $EuPW_{11}$ powder; (b) $EuPW_{11}$/PVA ultrafine fibers mats; (c) EuW_{10} powder; (d) EuW_{10}/PVA ultrafine fibers mats; (e) PVA ultrafine fibers mats.

TABLE I
FTIR Data (ν/cm^{-1}) of Solid and Ultrafine Fiber Mats

Sample	ν(P—O_a)	ν(W=O_d)	ν(W—O_b—W)	ν(W—O_c—W)
$EuPW_{11}$	1101, 1049	952	890	839, 769, 727
$EuPW_{11}$/PVA	1095, 1045	950	893	841, 779, 735
EuW_{10}		945	841	781, 700
EuW_{10}/PVA		933	845	783, 706

W_3O_{13} sets), O_c (edge-sharing oxygen-bridge within W_3O_{13} sets), and O_d (terminal oxygen atom). The IR data and assignment of solid and ultrafine fiber mats are listed in Table I. This demonstrate that the Eu-POMs polyanions are trapped in the ultrafine fiber mats and their chemical structures are not destroyed.[21] A more detailed inspection of the vibrational band shifts reveals that the bands of ν(P—O_a) and ν(W=O_d) bands of Eu-POMs in the ultrafine fiber mats have red shifts and the bands of ν(W—O_b—W) and ν(W—O_c—W) are blue-shifted compared with that of the pure solid. The shift of different peaks can be attributed to the presence of coulombic interaction between Eu-POMs and PVA.[14] In addition, at ca. 3400 cm^{-1}, O—H stretching vibration band of the Eu-POMs/PVA ultrafine fiber mats have red shifts and became broader than that of Eu-POMs solid. These results are owing to the presence of intermolecular bonding.[22]

UV–vis absorption spectra

Both the UV–vis absorption spectra of $EuPW_{11}$ aqueous solution and the $EuPW_{11}$/PVA ultrafine fiber mats exhibit a characteristic absorption band of $EuPW_{11}$ centered at ca. 250 nm corresponding to the $O_{b,c}$→W charge transfer (CT) transitions (Fig. 3),[23,24] which demonstrate $EuPW_{11}$ has been successfully incorporated with PVA fibers.[24,25] However, the characteristic absorption band of $EuPW_{11}$ in the ultrafine fiber mats is red-shifted from 251 to 253 nm. The wavelength shifts can be attributed to the interactions between $EuPW_{11}$ and PVA matrix, which influence the O→W charge transitions of europium-substituted heteropolytungstate.[25] The same conclusion can be obtained from the absorption spectra of EuW_{10} and EuW_{10}/PVA ultrafine fibers mats.

Fluorescence spectra

Figure 4 shows the excitation spectra of the Eu-POMs solid and the Eu-POMs/PVA ultrafine fiber mats at room temperature. The excitation spectra of Eu-POMs solid exhibit strong characteristic peaks of Eu^{3+} and a week broad band in ultraviolet region, which correspond to the ligand-metal charge transfer (LMCT) within polytungstate ligand.[26–28] However, the excitation spectra of Eu-POMs/PVA ultrafine fiber mats at room temperature only exhibit a strong broad band in ultraviolet region. Compared with the broad band, the characteristic bands of Eu^{3+} are so weak that hardly can be detected. The strong broad asymmetric band corresponding to the LMCT within the polytungstate ligand plays an important role in Eu-POMs luminescence. The photoexcitation of the LMCT band leads to intramolecular energy more efficiently transfer from polyanion to Eu^{3+}, followed by a characteristic luminescence of Eu^{3+}.[29,30]

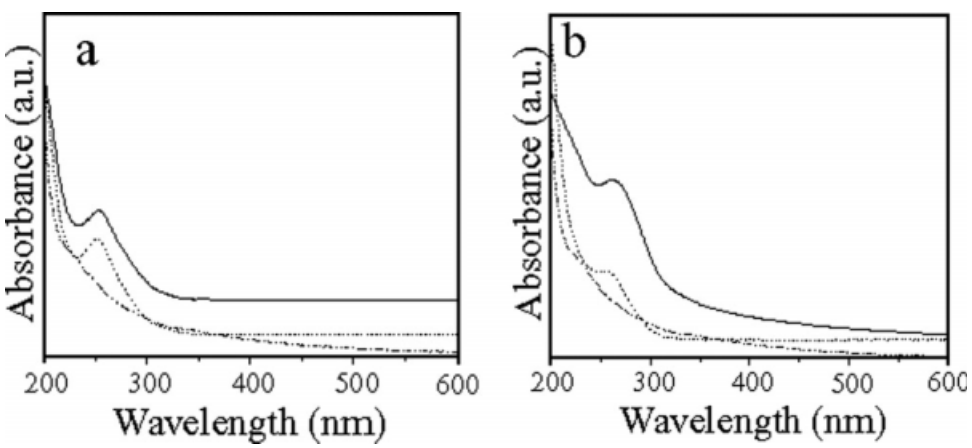

Figure 3 The UV–vis absorption spectra of Eu-POMs aqueous solution (dash line), Eu-POMs/PVA ultrafine fiber mats (solid line), and the PVA ultrafine fiber mats (dash dot line): (a) $EuPW_{11}$ and (b) EuW_{10}.

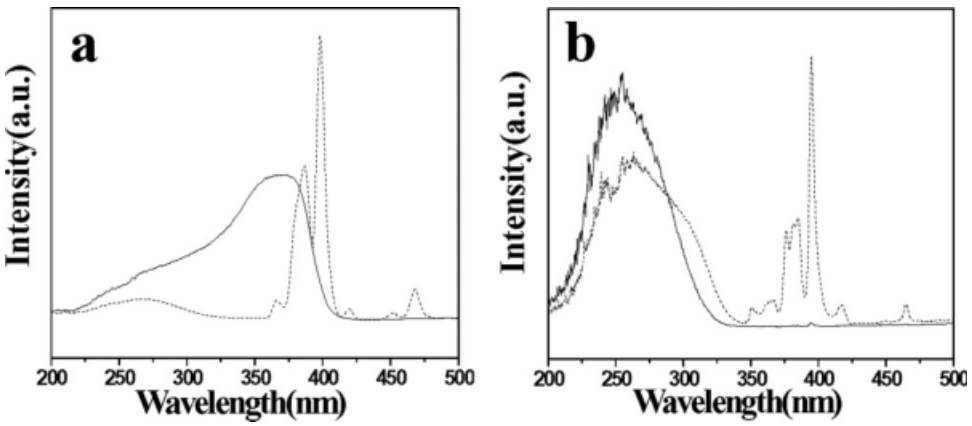

Figure 4 The excitation spectra of the Eu-POMs solid (dash line) and the Eu-POMs/PVA ultrafine fiber mats (solid line) at room temperature: (a) $EuPW_{11}$ and (b) EuW_{10}.

The emission spectra of Eu-POMs solid and Eu-POMs/PVA ultrafine fiber mats excited at 398, 370, 395, and 254 nm, respectively, show the characteristic transition of Eu^{3+} ion, as shown in Figure 5. These bands are due to transitions within the $4f^6$-electron shell and assigned to energy level transition from $^5D_0$ metastable state to terminal levels. They are attributed to $^5D_0 \rightarrow {}^7F_j$ (j=0, 1, 2, 3, 4) transitions.[31] The emission wavelengths with their assignments are listed in Table II. As we know, the $^5D_0 \rightarrow {}^7F_1$ transition is a magnetic dipole transition and its intensity varies with the crystal field strength acting on Eu^{3+}. On the other hand, the $^5D_0 \rightarrow {}^7F_2$ transition is an electric dipole transition and is extremely sensitive to chemical bonds in the vicinity of Eu^{3+}, so it was called hypersensitive transition. When Eu^{3+} is in a lattice with strict inversion centre, $^5D_0 \rightarrow {}^7F_1$ transitions will be main; while Eu^{3+} is in a lattice departured strict inversion centre, Laporte forbidden is broadened, and part of spin-forbidden f-f transitions will be relieved, then $^5D_0 \rightarrow {}^7F_2$ transitions will be appeared. The intensity of $^5D_0 \rightarrow {}^7F_2$ transition increases as the site symmetry of Eu^{3+} ion center decreases. Hence, the relative intensity ratio of the $^5D_0 \rightarrow {}^7F_2$ transition to the $^5D_0 \rightarrow {}^7F_1$ transition is widely used as a measure of the coordination state and the symmetry of rare earth.[30,32,33] For $EuPW_{11}$/PVA ultrafine fiber mats, there are obvious changes of some emission peaks compared with the $EuPW_{11}$ solid. In the emission spectrum of $EuPW_{11}$/PVA ultrafine fiber mats, we can observe a puny band at 579 nm, which is attributed to the $^5D_0 \rightarrow {}^7F_0$ transition, whereas it is not detected in the solid. It is well known that the $^5D_0 \rightarrow {}^7F_0$ transition is strictly forbidden in a field of symmetry. Hence, the presence of $^5D_0 \rightarrow {}^7F_0$ transition in the $EuPW_{11}$/PVA ultrafine fiber mats show that Eu^{3+} ion sites with low symmetry and without an inversion center.[34,35] In addition, the relative intensity ratio of the $^5D_0 \rightarrow {}^7F_2$ transition to $^5D_0 \rightarrow {}^7F_1$ transition is 7.08 in the $EuPW_{11}$/PVA ultrafine fiber mats and higher than 0.69 in the $EuPW_{11}$ solid. This result gives another evidence for lower site symmetry of Eu^{3+} in the ultrafine fiber mats. The site symmetry of Eu^{3+} in the ultrafine

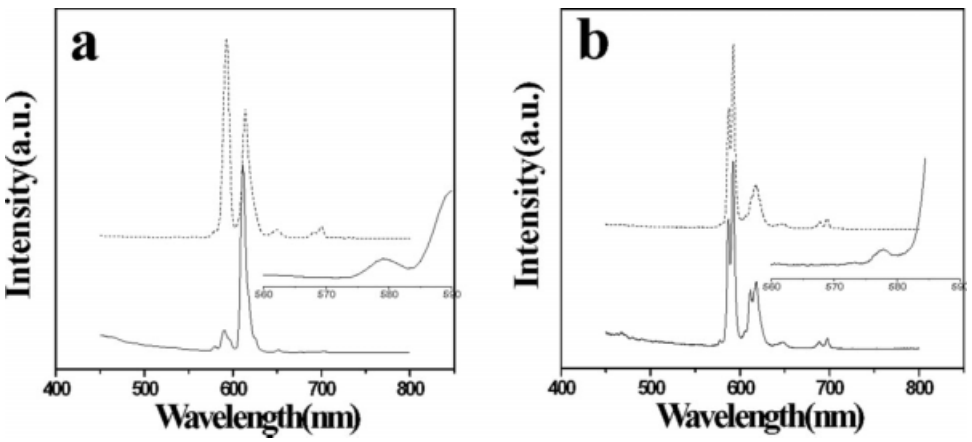

Figure 5 The emission spectra of the Eu-POMs solid (dash line) and the Eu-POMs/PVA ultrafine fiber mats (solid line) at room temperature: (a) $EuPW_{11}$ and (b) EuW_{10}.

TABLE II
Comparison of the Fluorescence Excitation and Emission Spectra of Solid and Ultrafine Fiber Mats

State	Excitation beam (nm)	$^5D_0 \rightarrow {}^7F_j$ ($j = 0-4$) emission (nm)				
		$j = 0$	$j = 1$	$j = 2$	$j = 3$	$j = 4$
$EuPW_{11}$	398		593	614	650	692, 700
$EuPW_{11}$/PVA	370	579	590	611	651	702
EuW_{10}	395		587, 592	606–618	649	688, 697
EuW_{10}/PVA	254	577	587, 592	606, 611, 618	649	688, 698

fiber mats is distorted possibly because that the strong electrostatic interaction between the matrix and $EuPW_{11}$ has an influence on the intensity of the crystal field acting on Eu^{3+}.[24] The same phenomena can be observed in the emission spectra of EuW_{10} and EuW_{10}/PVA ultrafine fibers mats (Fig. 5b). The $^5D_0 \rightarrow {}^7F_0$ transition, strictly forbidden by symmetry, only appears in EuW_{10}/PVA ultrafine fibers mats. The relative intensity ratio of the $^5D_0 \rightarrow {}^7F_2$ transition to the $^5D_0 \rightarrow {}^7F_1$ transition is 0.53 in the EuW_{10}/PVA ultrafine fiber mats a few higher than 0.28 in the EuW_{10} solid. These results also indicate the strong distortion of Eu^{3+} site symmetry in the EuW_{10}/PVA ultrafine fibers mats.

Compared the emission spectra of $EuPW_{11}$/PVA ultrafine fiber mats and EuW_{10}/PVA ultrafine fibers mats, which are obtained by the same way, the ratios of the relative intensity of the $^5D_0 \rightarrow {}^7F_2$ transition to the $^5D_0 \rightarrow {}^7F_1$ transition are different. The reason for this may be the dissimilar environments of the Eu^{3+}. The result also suggests that different interaction between polyanions and PVA matrix have different influence on the Eu^{3+} site symmetry. In $EuPW_{11}$, Eu^{3+} is coordinated by two PW_{11} groups through eight oxygen atoms forming an Archimedian antiprism. As known, PW_{11} group comes from PW_{12} losing a WO_6 octahedron. When two PW_{11} groups as ligand incorporate with Eu^{3+}, the symmetries of W—O_c—W and W—O_b—W stretch vibration decrease, which is due to Eu^{3+} incorporated with each PW_{11} group only by linking with two O_c atoms and two O_b atoms but not hold the position of W atom. Although in EuW_{10}, four oxygen atoms from the W_5O_{18} group of the half anion are bonded to the Eu atom, resulting in eightfold coordination of Eu^{3+}. The molecular structures of the products were shown in Figure 6. For Eu-POMs/PVA ultrafine fiber mats, the hydrogen bond is formed between PVA and end-oxygen polyanions, which can be observed from the IR spectra. The formation of hydrogen bond may change W—O—W and W—O—Eu bond angles and makes the intermolecular ligand environment asymmetry, with the influence of ligand electric field, the symmetry decreases as the polarity of Eu^{3+} increases. It also makes the $^5D_0 \rightarrow {}^7F_2$ transition increasing. Therefore, it is expected that in $EuPW_{11}$/PVA ultrafine fiber mats, more hydrogen bonds can be formed. It means that the crystal field strength acting on Eu^{3+} and chemical bonds in the vicinity of Eu^{3+} have great changes in $EuPW_{11}$/PVA ultrafine fiber mats compared with those of EuW_{10}/PVA ultrafine fiber mats. In other words, the site symmetry of Eu^{3+} is more strongly distorted in the $EuPW_{11}$/PVA ultrafine fiber mats.

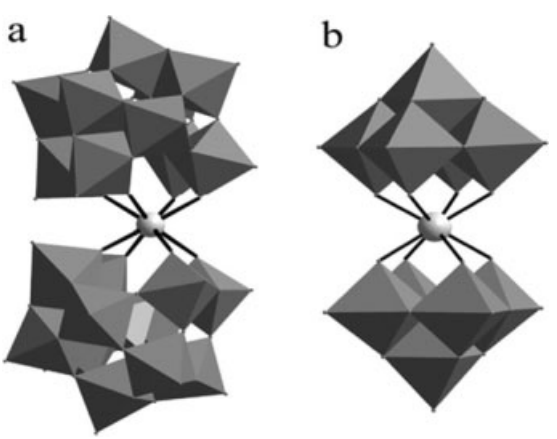

Figure 6 Molecular structures of $K_{11}[Eu(PW_{11}O_{39})_2]$ (a) and $Na_9[EuW_{10}O_{36}]$ (b).

CONCLUSIONS

In this article, we successfully prepared the ultrafine fiber mats based on europium-substituted heteropolytungstate via electrospinning method. The ultrafine fiber mats exhibited the characteristic emission bands of Eu^{3+}. The symmetric forbidden emission $^5D_0 \rightarrow {}^7F_0$ could be observed in the spectra of the Eu-POMs/PVA ultrafine fiber mats whereas this transition could not be found in the spectra of the Eu-POMs solid. At the same time, in the Eu-POMs/PVA ultrafine fiber mats, the intensity ratios of the $^5D_0 \rightarrow {}^7F_2$ transition to $^5D_0 \rightarrow {}^7F_1$ transition became larger. These results indicated the stronger interaction between the PVA matrix and heteropolytungstate and lower symmetry of the Eu^{3+} in the ultrafine fiber mats. On the other hand, the intensity ratio of the $^5D_0 \rightarrow {}^7F_2$ transition to $^5D_0 \rightarrow {}^7F_1$ transition was much larger in $EuPW_{11}$/PVA

ultrafine fiber mats than that in EuW_{10}/PVA ultrafine fiber mats. We presumed that the different configurations of $EuPW_{11}$ and EuW_{10} would be the main reason leading the different extent change on the Eu^{3+} site symmetry. This result also showed the pure red emission could be seen in $EuPW_{11}$/PVA ultrafine fiber mats. We hoped that the hybrid ultrafine fiber mats contained Ln-substituted POMs as optical, electrical, and magnetic materials had more widely applied foreground.

References

1. Liu, S. Q.; Kurth, D. G.; Bredenkotter, B.; Volkmer, D. J Am Chem Soc 2002, 124, 12279.
2. Kortz, U.; Vaissermann, J.; Thouvenot, R.; Gouzerh, P. Inorg Chem 2003, 42, 1135.
3. Wei, Y. G.; Lu, M.; Cheng, C. F.; Barnes, C.; Peng, Z. H. Inorg Chem 2001, 40, 5489.
4. Kortz, U.; Matta, S. Inorg Chem 2001, 40, 815.
5. Lu, Y.; Xu, Y.; Li, Y. G.; Wang, E. B.; Xu, X. X.; Ma, Y. Inorg Chem 2006, 45, 2055.
6. Zhang, C.; Howell, R. C.; Scotland, K. B.; Perez, F. G.; Todaro, L.; Francesconi, L. C. Inorg Chem 2004, 43, 7691.
7. Luo, Q. H.; Howell, R. C.; Bartis, J.; Dankova, M.; Horrocks, W. D.; Rheingold, A. L., Jr.; Francesconi, L. C. Inorg Chem 2002, 41, 6112.
8. Wang, X. L.; Wang, Y. H.; Hu, C. W.; Wang, E. B. Mater Lett 2002, 56, 305.
9. Xu, L.; Zhang, H. Y.; Wang, E. B.; Wu, A. G.; Li, Z. Mater Lett 2002, 54, 452.
10. Xu, L.; Zhang, H. Y.; Wang, E. B.; Wu, A. G.; Li, Z. Mater Chem Phys 2002, 77, 484.
11. Wang, Y. H.; Wang, X. L.; Hu, C. W. J. Colloid Interface Sci 2002, 249, 307.
12. Ito, T.; Yamase, T. J Alloys Compd 2006, 408, 813.
13. Wang, J.; Liu, F. Y.; Fu, L. S.; Zhang, H. J. Mate Lett 2002, 56, 300.
14. Zhang, H. Y.; Xu, L.; Wang, E. B.; Jing, M.; Wu, A. G.; Li, Z. Mater Lett 2003, 57, 1417.
15. Haraguchi, N.; Okaue, Y.; Isobe, T.; Matsuda, Y. Inorg Chem 1994, 33, 1015.
16. Peacock, R. D.; Weakley, T. J. R. J Chem Soc (A) 1971, 1836.
17. Liu, Y.; Ren, W.; Zhang, L. Y.; Yao, X. Thin Solid Films 1999, 353, 124.
18. Nicho, M. E.; Hu, H.; Energy, S. Mater Sol Cells 2000, 63, 423.
19. El-Kader, K. M.; Abd, A. S. Polym Test 2002, 21, 591.
20. Sousa, F. L.; Pillinger, M.; Ferreira, R. S.; Granadeiro, C. M.; Cavaleiro, A. M. V.; Rocha, J.; Carlos, L. D.; Trindade, T.; Nogueira, H. I. S. Eur J Inorg Chem 2006, 726.
21. Wu, H. D.; Wu, I. D.; Chang, F. C. Polymer 2001, 42, 555.
22. Shao, C. L.; Kim, H. Y.; Gong, J.; Ding, B.; Lee, D. R.; Park, S. J. Mater Lett 2003, 57, 1579.
23. Ma, H. Y.; Peng, J.; Han, Z. G.; Feng, Y. H.; Wang, E. B. Thin Solid Films 2004, 446, 161.
24. Wang, J.; Wang, H. S.; Fu, L. S.; Liu, F. Y.; Zhang, H. J. Thin Solid Films 2002, 414, 256.
25. Wang, Z.; Wang, J.; Zhang, H. J. Mater Chem Phys 2004, 87, 44.
26. Yamase, T.; Naruke, H. J. Chem Soc, Dalton Trans 1990, 1678.
27. Yamase, T.; Sugeta, M. J. Chem Soc, Dalton Trans 1993, 759.
28. Yamase, T.; Naruke, H. J. Chem Soc, Dalton Trans 1991, 285.
29. Yamase, T. Chem Rev 1998, 98, 307.
30. Zhang, T. R.; Lu, R.; Zhang, H. Y.; Xue, P. C.; Feng, W.; Liu, X. L.; Zhao, B.; Zhao, Y. Y.; Li, T. J.; Yao, J. N. J Mater Chem 2003, 13, 580.
31. Blasse, G.; Dirksen, G. J.; Zonnevijlle, F. J. J Inorg Nucl Chem 1981, 43, 2847.
32. Dejneka, M.; Snitzer, E.; Riman, R. E. J Non-Cryst Solids 1996, 202, 23.
33. Nogami, M.; Abe, Y. J Non-Cryst Solids 1996, 197, 73.
34. Richardson, F. S. Chem Rev 1982, 82, 541.
35. Zheng, Y. X.; Lin, J.; Liang, Y. J.; Yu, Y. N.; Zhou, Y. H.; Guo, C.; Wang, S. B.; Zhang, H. J. J Alloys Compd 2002, 336, 114.